

## PERSPECTIVE OPEN

## Environmental degradation of high-temperature protective coatings for ceramic-matrix composites in gas-turbine engines

Nitin P. Padture <sup>1</sup>

The need for higher efficiencies and performance in gas-turbine engines that propel aircraft in the air, and generate electricity on land, is pushing the operating temperatures of the engines to unprecedented levels. Replacing some of the current hot-section metallic components with ceramic-matrix composites (CMCs) is making that possible. A high-temperature ceramic coatings system, that includes environmental-barrier coatings (EBCs), are needed to protect CMCs. However, these coatings undergo degradation in the highly hostile environment of the gas-turbine engine consisting of a combination of high gas temperatures, pressures, and velocities. In addition, there is the ubiquitous presence of steam (a combustion by-product) and occasional ingestion of calcia-magnesia-aluminosilicates (CMASs) in the form of dust, sand, or ash from the environment. Steam can cause corrosion of EBCs, and the molten CMAS deposits can react with the EBCs resulting in their failure. This article provides a perspective on the understanding of these degradation mechanisms, and possible approaches, guided by that understanding, for mitigating the degradation. An outlook on the future challenges and opportunities is presented.

npj Materials Degradation (2019)3:11 ; <https://doi.org/10.1038/s41529-019-0075-4>

## CERAMIC ENVIRONMENTAL BARRIER COATINGS (EBCs)

Gas-turbine engines that propel aircraft and generate electricity have a huge impact on the transportation, energy, and defense sectors of the global economy.<sup>1</sup> It has been estimated that cumulative sales of gas-turbine engines in the period 2017–2031 will approach US\$2 trillion.<sup>2</sup> While current engines perform admirably and are highly efficient, there is always demand for even higher performance, better fuel efficiency, and lower NO<sub>x</sub> emissions. Typically, this can be accomplished by elevating the gas-inlet temperature in the hottest part (hot-section) of the gas-turbine engine, where the core-power and the efficiency scale with that temperature.<sup>1</sup> But the high-temperature capability of the current hot-section materials is the “bottleneck.” Improvements in superalloy, and the use of ceramic thermal barrier coatings (TBCs) in conjunction with internal air-cooling and air-film cooling of the superalloys components, have resulted in unprecedented gas-inlet temperatures in today's gas-turbine engines.<sup>1,3–5</sup> However, TBCs-coated superalloys are reaching their temperature-capability limit, and it is not clear if they will be able to achieve the >1700 °C gas-inlet temperature goal.<sup>1</sup> In this context, ceramic-matrix composites (CMCs) offer a “quantum jump” in temperature capability.<sup>1,6,7</sup> Gas-turbine engines with hot-section components made of CMCs, comprising continuous fibers and matrices made of SiC, are already in-service commercially, both for aircraft propulsion and electricity generation.

Unfortunately, SiC-based CMCs undergo active oxidation and recession in the high-temperature, high-pressure, high-velocity gas stream of the gas-turbine engine which invariably contains steam, a combustion by-product.<sup>8,9</sup> Thus, dense, crack-free environmental barrier coatings (EBCs) are needed to protect SiC-based CMCs from this environmental degradation by blocking diffusion/ingression of oxygen/steam.<sup>1,10–13</sup> For achieving crack-free EBCs, they must have an excellent coefficient of thermal

expansion (CTE) match with SiC-based CMCs ( $\sim 4.5 \times 10^{-6} \text{ }^\circ\text{C}^{-1}$ ), which limits the choice of ceramics that can be used as EBCs.<sup>1,12–14</sup> EBCs must also have low volatility for minimizing steam-induced corrosion/recession, and be resistant to degradation by molten calcia-magnesia-aluminosilicate (ingested dust, sand, or ash; commonly referred to as CMAS) deposits, among several other requirements, including high-temperature capability; phase stability; chemical compatibility with other layers; and mechanical robustness (high hardness and toughness) against fracture, erosion, and impact-damage.<sup>1,12–14</sup> Since the failure of EBCs will result in the catastrophic degradation of the CMCs, EBCs need to be prime-reliant. EBCs also need to be readily manufacturable using commercially available scalable methods such as those based on thermal spray.

Research on EBCs began in earnest in the late 1990s, soon after the discovery of active high-temperature oxidation of SiC in steam environment.<sup>12,13</sup> Since typical refractory oxide structural ceramics such as Al<sub>2</sub>O<sub>3</sub> and ZrO<sub>2</sub> have a high CTE ( $\sim 10 \times 10^{-6} \text{ }^\circ\text{C}^{-1}$ ), they are not suitable for EBC application. Initially, (1-x)BaO·xSrO·Al<sub>2</sub>O<sub>3</sub>·2SiO<sub>2</sub> (0 < x < 1; BSAS) ceramics with lower CTE ( $\sim 4.3 \times 10^{-6} \text{ }^\circ\text{C}^{-1}$ , Celsius phase) were considered, where a typical EBC structure (Fig. 1a) comprised three layers: Si bond-coat, BSAS/mullite inter-layer, and BSAS top-coat.<sup>12,15</sup> All these layers are typically deposited using thermal-spray methods. Since oxide coatings typically do not bond well to the non-oxide CMC, the Si bond-coat is necessary. It also provides oxidation protection to the CMC by forming a dense, slow-growing SiO<sub>2</sub> thermally-grown oxide (TGO) layer. As the temperature requirements have increased, EBCs based on rare-earth (RE) monosilicates (RESi<sub>2</sub>O<sub>5</sub>), disilicates (RE<sub>2</sub>Si<sub>2</sub>O<sub>7</sub>), and their variations, are being developed.<sup>12,13</sup> While most RE<sub>2</sub>Si<sub>2</sub>O<sub>7</sub> ceramics have a better CTE match with SiC, they have higher SiO<sub>2</sub> activity relative to RE<sub>2</sub>SiO<sub>5</sub>, and are more prone to volatilization in steam.<sup>12</sup> Since EBCs are expected

<sup>1</sup>School of Engineering, Brown University, Providence, RI 02912, USA

Correspondence: Nitin P. Padture ([nitin\\_padture@brown.edu](mailto:nitin_padture@brown.edu))

Received: 31 December 2018 Accepted: 4 March 2019

Published online: 15 March 2019

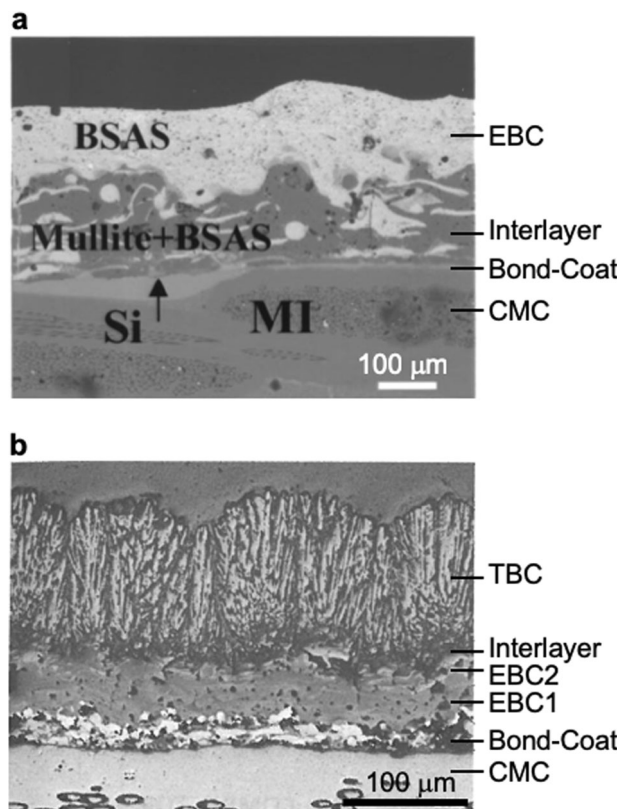


**Fig. 1** Coating-systems for CMCs. **a** Cross-sectional SEM image of BSAS/BSAS+Mullite/Si EBC on melt-infiltrated (MI) CMC. **b** Cross-sectional optical micrograph of multilayer T/EBC on CMC. (**a**, **b** reproduced/adapted with permission from refs <sup>13,15</sup>, respectively. Copyright John Wiley & Sons Inc. 2003 and 2016.)

to be prime-reliant, and the ultimate failure of EBCs is mechanical,  $\text{RE}_2\text{Si}_2\text{O}_7$  ceramics appear to be a better choice for EBCs. Further increase in the high-temperature requirements (up to 1700 °C) is necessitating the use of an additional thermally-insulating top-coat (TBC), in the so-called thermal/environmental barrier coatings (T/EBCs) (Fig. 1b), in conjunction with cooling of the CMC component.<sup>13,16,17</sup>  $\text{ZrO}_2$ -based and  $\text{HfO}_2$ -based TBCs are being considered for that application.<sup>13,16,17</sup> However, the CTEs of these TBCs are considerably higher, requiring the use of an intermediate layer between the EBC and the TBC. Most recently, the use of a single layer (TEBC), to replace the three layers, is proposed, one made of solid-solution  $\text{RE}_x\text{RE}'_{(2-x)}\text{Si}_2\text{O}_7$  disilicate ceramics with low thermal conductivity and good CTE match with SiC.<sup>18</sup> Regarding the bond-coat, Si melts at 1416 °C, hence new bond-coat materials, such as silicides and particulate nanocomposites, with higher temperature capabilities are being investigated.<sup>13</sup> Alternatively, coating systems free of bond-coat are also being explored.

Since currently there is no coating system that meets all the operating-temperature goals adequately, the EBCs research field is very active globally. However, while some of the research performed in this field is in the public domain, much of the research and development work remains highly proprietary.

### STEAM-INDUCED DEGRADATION AND MITIGATION

SiC-based CMCs oxidize at high temperatures to produce a  $\text{SiO}_2$  TGO passivating layer according to the following reaction:<sup>19</sup>

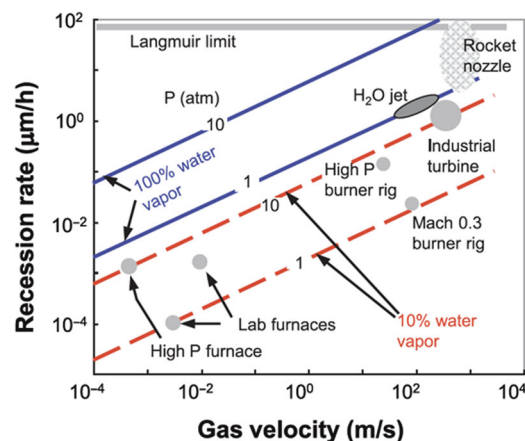
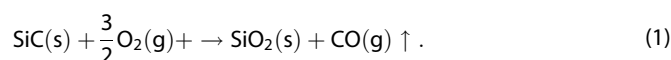


**Fig. 2** Steam-induced corrosion of SiC. Recession rate of SiC in flowing water vapor (blue solid lines) and in hydrocarbon combustion (red broken lines, 10% water vapor) at 1316 °C, assuming laminar flow over a flat plate and volatilization of  $\text{Si}(\text{OH})_4$ . Conditions corresponding to several test facilities, including the high-speed water vapor jet, are indicated and compared with typical conditions for industrial turbine engines and rocket nozzles. (Figure reproduced with permission from ref. <sup>20</sup>. Copyright John Wiley & Sons Inc. 2011.)

However, as mentioned earlier, the high-temperature, high-pressure, high-velocity gas stream of the gas-turbine engines always contains steam, which results in the active volatilization of the TGO, according to the following reaction, and the rapid recession of SiC.<sup>8</sup>

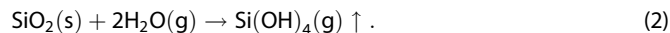
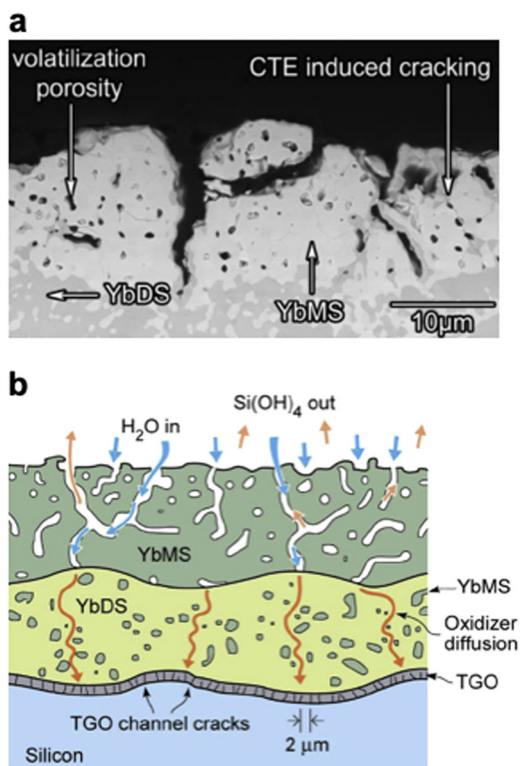


Figure 2 presents a map of SiC-recession rate and gas velocity ( $v$ ) for various  $\text{H}_2\text{O}$  partial pressures ( $P_{\text{H}_2\text{O}}$ ), and total pressure ( $P$ ) conditions (at 1316 °C),<sup>20</sup> where the recession rate is proportional to  $(v^{0.5} P_{\text{H}_2\text{O}}^2 P^{-0.5})$ .<sup>8</sup> Thus, recession rates of as high as  $\sim 1 \mu\text{m h}^{-1}$  are observed under gas-turbine engine operating conditions ( $v \sim 300 \text{ m s}^{-1}$ ,  $P_{\text{H}_2\text{O}} \sim 0.1$ ,  $P \sim 10 \text{ atm}$ ).<sup>20</sup>

EBCs are expected to have significantly lower recession rates due the reduced  $\text{SiO}_2$  activity ( $a_{\text{SiO}_2}$ ) in those ceramics, where the recession rate is determined by the flux of  $\text{Si}(\text{OH})_4(\text{g})$  in Reaction 2, which is directly proportional to  $a_{\text{SiO}_2}$ . For example, the ideal  $a_{\text{SiO}_2}$  in BSAS is 0.5, but experimentally it has been measured to be as low as  $\sim 0.1$ , making BSAS resistant to steam corrosion.<sup>12</sup> Regarding RE-silicates, the ideal  $a_{\text{SiO}_2}$  for RE-monosilicates and RE-disilicates is 0.33 and 0.5, respectively. In this context,  $a_{\text{SiO}_2}$  values in certain phase regions in  $\text{Y}_2\text{O}_3\text{-SiO}_2$  and  $\text{Yb}_2\text{O}_3\text{-SiO}_2$  phase diagrams have been measured as a function of temperature.<sup>21,22</sup> In the  $(\text{Y}_2\text{O}_3 + \text{Y}_2\text{SiO}_5)$  phase region  $a_{\text{SiO}_2}$  is estimated at  $\sim 0.0005$ , with a mild temperature dependence in the range 1265–1400 °C.<sup>21</sup> In the  $(\text{Y}_2\text{SiO}_5 + \text{Y}_2\text{Si}_2\text{O}_7)$  phase region  $a_{\text{SiO}_2}$  is estimated at  $\sim 0.32$  independent of temperature.<sup>21</sup> In the  $(\text{Yb}_2\text{O}_3 + \text{Yb}_2\text{SiO}_5)$  and  $(\text{Yb}_2\text{SiO}_5 + \text{Yb}_2\text{Si}_2\text{O}_7)$  phase regions,  $a_{\text{SiO}_2}$  is estimated at  $\sim 0.003$  and  $\sim 0.35$ , respectively, with mild temperature dependencies.<sup>22</sup> Such measurements are very valuable as they can be used to determine the efficacy of the EBCs in resisting steam-induced corrosion in the gas-turbine engine environment. It should be noted that, unlike SiC, EBCs do not recede uniformly. Instead, there is the formation of undesirable  $\text{SiO}_2$ -lean phases and porous microstructures, typically due to selective high-temperature steam-induced corrosion (see e.g., Figure 3).

Generally, the more stable the RE-silicate, i.e., more negative enthalpy of formation, the lower the  $a_{\text{SiO}_2}$  and more resistant it is to steam-induced corrosion.<sup>22</sup> While the ionization potentials,  $Z/r$  ( $Z$  = atomic number,  $r$  = ionic radius), of the binary RE-oxides can be used as a rough guide to rank the relative stability of respective



**Fig. 3** Steam-induced degradation of an EBC. **a** Cross-sectional SEM image of  $\text{Yb}_2\text{Si}_2\text{O}_7$  (YbDS) EBC subjected to furnace steam-cycling (each cycle: 60 min hot at 1326 °C, 10 min cold at 110 °C) for 2000 cycles ( $v = 0.044 \text{ m s}^{-1}$ ,  $P_{\text{H}_2\text{O}} = 0.9$ ,  $P \sim 1 \text{ atm}$ ). The top surface of the EBC has transformed to  $\text{Yb}_2\text{SiO}_5$  (YbMS) due to  $\text{SiO}_2$  depletion. **b** Schematic illustration of steam-induced degradation of YbDS EBC. (**a**, **b** reproduced with permission from ref. <sup>14</sup>. Copyright Elsevier 2016.)

RE-silicates,<sup>23</sup> it has limitations due to the complex chemistries of RE-silicates that contain multiple cations. In this context, it has been suggested that a more useful parameter that indicates the relative stability of a RE-silicate, while capturing its complex chemistry, is its optical basicity (OB or  $\Lambda$ ).<sup>22</sup> OB of a binary metal-oxide is defined as the measure of oxygen anion's ability to donate electrons, which depends on the polarizability of the metal cations.<sup>24,25</sup> Cations with low polarizability have high OBs, and they are generally more stable.<sup>26</sup> The OB values of several binary oxides are known, but importantly, OBs of multi-cation oxides can be calculated using the following relation:<sup>25</sup>

$$\Lambda = X_A \Lambda_A + X_B \Lambda_B + X_C \Lambda_C + \dots \quad (3)$$

where  $X_A$ ,  $X_B$ ,  $X_C$ ... are the fractions of oxygen ions contributed by the respective oxides (A, B, C...) to the system, and  $\Lambda_A$ ,  $\Lambda_B$ ,  $\Lambda_C$ ... are the OBs of the respective oxides. For example, OBs of  $\text{Y}_2\text{SiO}_5$ ,  $\text{Y}_2\text{Si}_2\text{O}_7$ ,  $\text{Yb}_2\text{SiO}_5$ , and  $\text{Yb}_2\text{Si}_2\text{O}_7$  are calculated to be 0.79, 0.70, 0.76, and 0.68, respectively.<sup>27</sup> While there is early indication that Y-silicates, with their higher OBs compared to their Yb-silicate counterparts, are more resistant to steam-induced corrosion,<sup>22</sup> it remains to be seen if this simplified correlation is valid across all RE-silicates and their alloys.

This brings us to the issue of testing of steam-induced corrosion of EBCs. First, instead of actual EBCs, most often polycrystalline sintered EBC ceramics are tested because they are easier to fabricate.<sup>28,29</sup> Since EBCs are supposed to be dense, the sintered EBC ceramics are a good proxy material to test. However, in some studies, the sintered EBC ceramics are not fully dense, which can result in exaggerated steam-induced corrosion. In studies where thermal-sprayed EBCs are used, they can have variable porosity

level, chemical/phase composition, and crystallinity. Second, majority of the studies are performed in an atmospheric pressure tube furnace under low-velocity flowing air (or another carrier gas) with steam, where weight change and/or recession rate is measured.<sup>9</sup> These conditions are denoted by "lab furnaces" in Fig. 2, and they are far from what exist in gas-turbine engines ("industrial turbine" in Fig. 2). Also, the tube material can complicate the results. For example, when fused  $\text{SiO}_2$  tubes are used, they themselves corrode, resulting in artificially high  $\text{Si}(\text{OH})_4$  vapor pressure and an attendant slowdown of the steam-induced corrosion of the test pieces.<sup>29</sup> On the other hand, the use of  $\text{Al}_2\text{O}_3$  tubes results in  $\text{Al}(\text{OH})_3$  contamination and deposition on the test pieces.<sup>29</sup> Third, a wide variety of  $\text{H}_2\text{O}$  vapor pressure and temperature conditions are used in the various studies. While some insights into the degradation mechanisms can be gained from these studies (e.g., Figure 3), all these factors make it very difficult to compare results between the various studies, and in some cases can lead to wrong conclusions.

In this context, burner-rig-based tests approach gas-turbine engine conditions ( $v = 100 \text{ m s}^{-1}$ ,  $P_{\text{H}_2\text{O}}$  range 0.1–0.25,  $P = 1 \text{ atm}$ ,  $T$  range 1200–1500 °C), but they are quite expensive to run.<sup>30</sup> More recently, tests involving the use of capillary steam-jet impinging on the test piece surface, inside a furnace, have been used, achieving steam  $v$  in the ranges 40–260  $\text{m s}^{-1}$ .<sup>20,31,32</sup> Although the furnace is at atmospheric pressure ( $P = 1 \text{ atm}$ ), the  $P_{\text{H}_2\text{O}} = 1$ , which is higher than that in burner-rig tests, results in the equivalent steam-jet test conditions approaching gas-turbine engine conditions (Fig. 2). Some of the issues with the steam-jet testing is that the capillaries, which are made of glass, quartz or mullite, can themselves corrode and contaminate the steam jet. Recently, Opila and co-workers have used noble-metal capillary tubes to mitigate this issue. However, the corroded areas in steam-jet tests are still highly localized and small in size ( $\sim \text{mm}^2$ ). Thus, it is not clear how the results from these tests may correlate with the steam-induced corrosion that can occur over large areas of hot-section components in a gas-turbine engine. Most recently, Vaßen and co-workers have developed a new method that addresses some these concerns, where a high-velocity oxy-fuel (HVOF) torch is used to generate 100%  $\text{H}_2\text{O}$  atmosphere in situ ( $P = 1 \text{ atm}$ ), with velocities ( $v$ ) reaching up to 1000  $\text{m s}^{-1}$ , over relatively large areas ( $\sim \text{cm}^2$ ).

Thus, there is a clear need for standardizing the testing of steam-induced corrosion of EBC ceramics and EBCs to gain a better, and more relevant, understanding of the mechanisms. This will provide a more meaningful comparison between the different EBC ceramics and microstructures, and guidance for tailoring them for future EBCs with superior resistance to steam-induced corrosion.

The TBC top-coats in T/EBCs are typically made of  $\text{ZrO}_2$ -based and/or  $\text{HfO}_2$ -based ceramics and are Si-free ( $a_{\text{SiO}_2} = 0$ ).<sup>13,16,17</sup> Thus, they may not be prone to severe steam-induced corrosion, but the thermal-barrier top-coats are porous, which allows the high-pressure steam to access the underlying EBC layer. However, that access is limited, and also the EBC layer is not expected to experience the full brunt of the high-velocity, steam-laden gas stream, which represents a significant advantage of T/EBCs. The proposed single-layer TEBCs<sup>18</sup> will, unfortunately, not have that advantage.

### CMAS-INDUCED DEGRADATION AND MITIGATION

Another source of major high-temperature degradation of EBCs is due to CMAS, which is ingested occasionally in the form of airborne sand, runway debris, or volcanic ash by aircraft engines, and ambient dust and/or fly ash by electricity-generation engines.<sup>1,12,33</sup> Since most CMASs melt at temperatures  $\leq 1200$  °C, and the surface temperatures of EBCs are expected to be 1500 °C or higher, the CMAS deposits on EBCs as a molten glassy layer. The

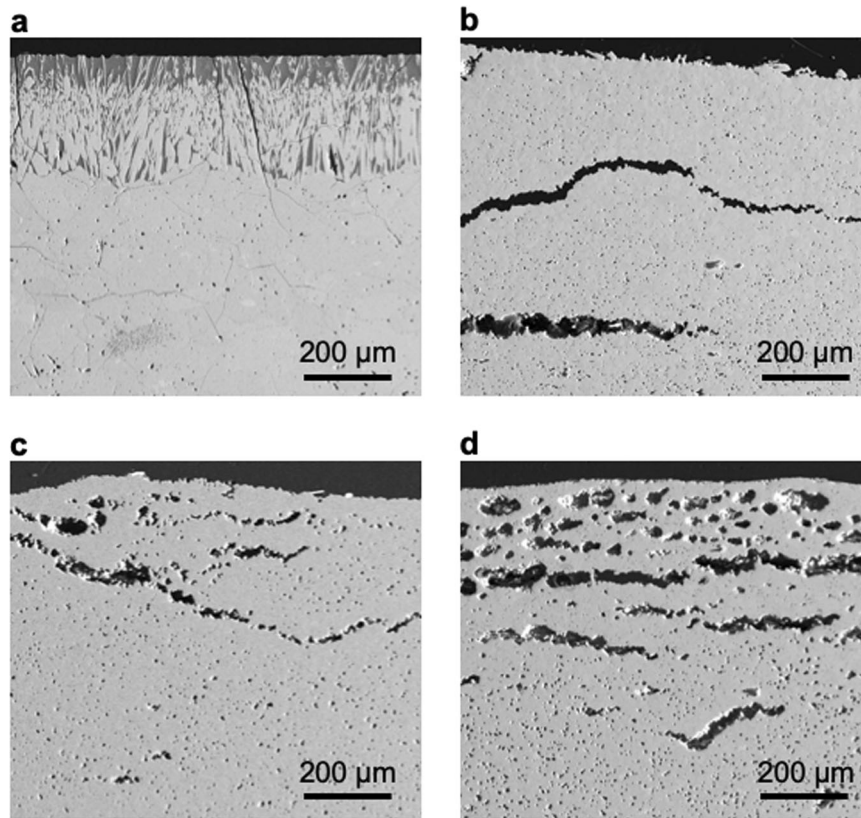


**Fig. 4** CAMS-induced degradation of EBC ceramics. Cross-section SEM images of dense, polycrystalline  $\text{RE}_2\text{Si}_2\text{O}_7$  ceramic pellets that have interacted with a CMAS glass under identical conditions ( $1500^\circ\text{C}$ , 24 h): **a**  $\text{Y}_2\text{Si}_2\text{O}_7$ , **b**  $\text{Yb}_2\text{Si}_2\text{O}_7$ , **c**  $\text{Sc}_2\text{Si}_2\text{O}_7$ , and **d**  $\text{Lu}_2\text{Si}_2\text{O}_7$ . (**a–d** reproduced with permission from ref. <sup>18</sup>. Copyright Elsevier 2018.)

degradation is primarily in the form of EBC/CMAS reaction, resulting in the formation of reaction products with uncontrolled microstructures and undesirable properties, such as high CTE and low toughness, leading to eventual failure of the EBC.<sup>1,12,33</sup> The molten-CMAS attack of EBC-coated CMCs is expected to be much more severe compared to that of TBC-coated superalloys because of the significantly higher operating temperatures in the latter (by up to  $300^\circ\text{C}$ ), and that all the relevant processes (diffusion, reaction, dissolution, viscosity, etc.) are thermally-activated. CMAS-resistant TBCs are designed to react with the CMAS and crystallize it, preventing the CMAS from penetrating into open porosity of the TBCs.<sup>1,33,34</sup> In contrast, EBCs are dense, and therefore, it is preferred that they have low or no reactivity with the CMAS to retain the EBC's integrity.<sup>1,18,33</sup> However, the CMASs can have a wide range of compositions depending on the source,<sup>27,34</sup> making it challenging to design non-reactive EBCs. Thus, CMASs that are most relevant to a certain situation are typically used in published studies.

The interaction of plasma-sprayed BSAS-based EBCs and a CMAS (sand) has been studied in some detail (at  $1300^\circ\text{C}$  for various durations).<sup>35</sup> It is found that the BSAS-based EBC reacts with the molten CMAS glass, resulting in its dissolution and reprecipitation as a modified Ca-containing celcian phase, with evidence for the formation of additional phases such as anorthite ( $\text{CaAl}_2\text{Si}_2\text{O}_8$ ).<sup>35</sup> The interaction of some of the newer EBC compositions, primarily RE-disilicates (mostly sintered pellets), with CMAS has also been reported in the literature:  $\text{Y}_2\text{Si}_2\text{O}_7$ ,<sup>36–39</sup>  $\text{Yb}_2\text{Si}_2\text{O}_7$ ,<sup>16,36,37,40–43</sup>  $\text{Sc}_2\text{Si}_2\text{O}_7$ ,<sup>36,43</sup> and  $\text{Lu}_2\text{Si}_2\text{O}_7$ .<sup>18,36</sup> However, direct comparisons are difficult because different CMAS compositions are used, and EBCs (or sintered pellets) have variable porosities/microstructures. Also, the heat-treatment temperatures, durations, and atmospheres (without or with steam) can vary from

study to study. However, here are some general observations that can be made. Typically,  $\text{Y}_2\text{Si}_2\text{O}_7$  reacts with most CMASs, resulting in the formation of reprecipitated  $\text{Y}_2\text{Si}_2\text{O}_7$  and Y-Ca-Si apatite solid-solution (ss) as the primary reaction products. In the case of  $\text{Yb}_2\text{Si}_2\text{O}_7$ , some studies have reported extensive reaction and the formation of Yb-Ca-Si apatite(ss) reaction product mainly, while others report minimal reaction but penetration of the CMAS along grain boundaries.<sup>43</sup> The latter can result in other type of damage such as “blister” cracking within the EBC ceramics (sintered pellets).<sup>43</sup> Similar observations have been made in  $\text{Sc}_2\text{Si}_2\text{O}_7$  and  $\text{Lu}_2\text{Si}_2\text{O}_7$  EBC ceramics.<sup>18,43</sup> Figure 4 shows the varied interactions of RE-disilicate EBC ceramics (sintered pellets) with sand CMAS ( $1500^\circ\text{C}$ , 24 h).<sup>18</sup> Thus, EBCs that do not react with CMAS, may encounter other types of damage mechanisms. But, once again, it will depend on the CMAS composition, EBC microstructure, and thermal-cycling conditions. CMAS-attack and mitigation approaches for T/EBCs will be similar to those for TBCs, except higher temperatures ( $\geq 1500^\circ\text{C}$ ) will need to be considered.<sup>16,17</sup>

In this context, an initial screening criterion for choosing CMAS-resistant EBC ceramics was introduced—small OB difference between CMAS and a given EBC ceramic.<sup>27</sup> The basis for this criterion is that at the Lewis acid-base chemistry level the reactivity between a crystalline oxide ceramic and an oxide glass is expected to decrease with decreasing difference between their OBs. Based on this simple criterion the following EBC ceramics are expected to be CMAS-resistant:  $\text{YAlO}_3$ ,  $\text{Y}_2\text{Si}_2\text{O}_7$ ,  $\text{Yb}_2\text{Si}_2\text{O}_7$ ,  $\text{Sc}_2\text{Si}_2\text{O}_7$ , and  $\text{Lu}_2\text{Si}_2\text{O}_7$ .<sup>18,27,38,43</sup> It should be emphasized that the OBs-difference analysis provides a rough screening criterion based on purely chemical considerations, and that the actual reactivity will depend on various factors including the nature of the cations in the EBC ceramics and the CMAS, and the stability of the reaction products.<sup>33</sup> The fact that  $\text{Y}_2\text{Si}_2\text{O}_7$  reacts with certain CMAS despite

having a small OB difference echoes this caveat.<sup>38</sup> Also, the “no-reaction-with-CMAS” criterion needs to be reexamined in light of new, unexpected damage mechanisms, such as “blister” cracking mentioned earlier, in non-reacting EBC ceramics. In this context, the omnipresent steam in the gas-turbine engine atmosphere can also influence the nature of the CMAS-induced degradation EBCs, but it has not been investigated in any detail. For example, it is known that high-temperature steam-induced corrosion of the CMAS deposits on top of EBCs can result in SiO<sub>2</sub>-depletion in the CMAS. Depending on the composition of the original CMAS, it can either trigger CMAS-layer crystallization making it more benign, or reduce the CMAS viscosity making it more dangerous. Thus, systematic studies of these highly dynamic combined effects under conditions in actual gas-turbine engine are needed. In summary, mitigation of CMAS-attack of EBCs will rely on gaining a basic understanding of the multi-faceted degradation mechanisms, and on using that understanding to design robust approaches.

## OUTLOOK

CMCs are likely to be ubiquitous in future high-performance, high-efficiency gas-turbine engines for aircraft propulsion and electricity-generation. Thus, effective, reliable, and manufacturable high-temperature ceramic-coating systems, including EBCs, T/EBCs, TBCs, etc., are needed urgently to protect CMCs from some of the most hostile environments that will exist in future gas-turbine engines, and help CMCs reach their full potential. However, the degradation of these coating systems by the various environmental factors, and their attendant thermo-chemo-mechanical failure, remains a major hurdle. While the discussion in this article is limited to degradation induced by steam and CMAS individually, their combined effects, together with consideration of other degradation modes, will become important. Thus, the understanding of all the interrelated degradation and failure mechanisms is key to making progress in this field. This will help guide the design, processing, testing, and implementation of suitable high-temperature ceramic-coating systems for CMCs in future gas-turbine engines, and it is expected to be a fruitful and impactful area of research for years to come.

## ACKNOWLEDGEMENTS

The author thanks A.R. Krause, D.B. Marshall, E.J. Opila, S. Sampath, L.R. Turcer, and R. Vaßen for fruitful discussions, and the Office of Naval Research and the Department of Energy for the financial support.

## AUTHOR CONTRIBUTIONS

N.P.P. wrote the manuscript.

## ADDITIONAL INFORMATION

**Competing interests:** The author declares no competing interests.

**Publisher's note:** Springer Nature remains neutral with regard to jurisdictional claims in published maps and institutional affiliations.

## REFERENCES

- Padture, N. P. Advanced structural ceramics in aerospace propulsion. *Nat. Mater.* **15**, 804–809 (2016).
- Alibrandi, W. Forecast international predicts tremendous world growth for gas turbines over next 15 years, [www.forecastinternational.com/press/release.cfm?article=13049#.VvV59kuv9e9](http://www.forecastinternational.com/press/release.cfm?article=13049#.VvV59kuv9e9) (2014).
- Padture, N. P., Gell, M. & Jordan, E. H. Thermal barrier coatings for gas-turbine engine applications. *Science* **296**, 280–284 (2002).
- Clarke, D. R., Oechsner, M. & Padture, N. P. Thermal-barrier coatings for more efficient gas-turbine engines. *MRS Bull.* **37**, 891–898 (2012).
- Darolia, R. Thermal barrier coating technology: critical review, progress update, remaining challenges and prospects. *Int. Mater. Rev.* **58**, 315–348 (2013).
- DiCarlo, J. A. in *Ceramic Matrix Composites: Materials, Modelling, and Technology* (eds Bansal, N. P. & Lamon, J.) 217–235, (Wiley, Hoboken, 2016).
- Zok, F. W. Ceramic-matrix composites enable revolutionary gains in turbine engine efficiency. *Am. Ceram. Soc. Bull.* **95**, 22–28 (2016).
- Opila, E. J. & Hann, R. Paralineer oxidation of CVD SiC in water vapor. *J. Am. Ceram. Soc.* **80**, 197–205 (1997).
- Meschter, P. C., Opila, E. J. & Jacobson, N. S. Water-vapor-mediated volatilization of high-temperature materials. *Ann. Rev. Mater. Sci.* **43**, 559–588 (2013).
- Lee, K. N. Current status of environmental barrier coatings for Si-based ceramics. *Surf. Coat. Technol.* **133–134**, 1–7 (2000).
- Lee, K. N., Fox, D. S. & Bansal, N. P. Rare earth silicate environmental barrier coatings for SiC/SiC composites and Si<sub>3</sub>N<sub>4</sub> ceramics. *J. Eur. Ceram. Soc.* **25**, 1705–1715 (2005).
- Lee, K. N. in *Ceramic Matrix Composites: Materials, Modeling and Technology* (eds Bansal, N. P. & Lamon, J.) 430–451 (Wiley, Hoboken, 2015).
- Zhu, D. in *Engineered Ceramics: Current Status and Future Prospects* (eds Ohji, T. & Singh, M.) 187–202 (Wiley, Hoboken, 2016).
- Richards, B. T. et al. Response of ytterbium disilicate-silicon environmental barrier coatings to thermal cycling in water vapor. *Acta Mater.* **106**, 1–14 (2016).
- Lee, K. N. et al. Upper temperature limit of environmental barrier coatings based on mullite and BSAS. *J. Am. Ceram. Soc.* **86**, 1299–1306 (2003).
- Poerschke, D. L. et al. Stability and CMAS resistance of ytterbium-silicate/hafnate EBC/TBC for SiC composites. *J. Am. Ceram. Soc.* **98**, 278–286 (2015).
- Krause, A. R., Garcés, H. F., Herrmann, C. E. & Padture, N. P. Resistance of 2ZrO<sub>2</sub>-Y<sub>2</sub>O<sub>3</sub> top coat in thermal/environmental barrier coatings to calcia-magnesia-aluminosilicate attack at 1500 °C. *J. Am. Ceram. Soc.* **100**, 3175–3187 (2017).
- Turcer, L. R. & Padture, N. P. Towards multifunctional thermal environmental barrier coatings (TEBCs) based on rare-earth pyrosilicate solid-solution ceramics. *Scr. Mater.* **154**, 111–117 (2018).
- Jacobson, N. S. Corrosion of silicon-based ceramics in combustion environment. *J. Am. Ceram. Soc.* **76**, 3–28 (1993).
- dos Santos e Lucato, S. L., Sudre, O. H. & Marshall, D. B. A method for assessing reactions of water vapor with materials in high-speed, high-temperature flow. *J. Am. Ceram. Soc.* **94**, S186–S195 (2011).
- Jacobson, N. S. Silica activity measurements in the Y<sub>2</sub>O<sub>3</sub>-SiO<sub>2</sub> system and applications to modeling of coating volatility. *J. Am. Ceram. Soc.* **97**, 1959–1965 (2014).
- Costa, G. C. C. & Jacobson, N. S. Mass spectrometric measurements of the silica activity in the Yb<sub>2</sub>O<sub>3</sub>-SiO<sub>2</sub> system and implications to assess the degradation of silicate based coatings in combustion environments. *J. Eur. Ceram. Soc.* **35**, 4259–4267 (2015).
- Navrotsky, A. Repeating patterns in mineral energetics. *Am. Mineral.* **79**, 589–605 (1994).
- Duffy, J. A. & Ingram, M. D. An interpretation of glass chemistry in terms of the optical basicity concept. *J. Non-Cryst. Solids* **21**, 373–410 (1976).
- Duffy, J. A. Acid-base reactions of transition metal oxides in the solid state. *J. Am. Ceram. Soc.* **80**, 1416–1420 (1997).
- Nanba, T., Miura, Y. & Sakida, S. Consideration of the correlation between basicity of oxide glasses and O1s chemical shift in XPS. *J. Ceram. Soc. Jpn* **113**, 44–50 (2005).
- Krause, A. R. et al. 2ZrO<sub>2</sub>-Y<sub>2</sub>O<sub>3</sub> thermal barrier coatings resistant to degradation by molten CMAS: part I, optical basicity considerations and processing. *J. Am. Ceram. Soc.* **97**, 3943–3949 (2014).
- Klemm, H., Fritsch, M. & Schenk, B. Corrosion of ceramic materials in hot gas environment. *Ceram. Eng. Sci. Proc.* **25**, 463–468 (2004).
- Maier, N., Nickel, K. G. & Rixecker, G. High temperature water vapour corrosion of rare earth disilicates (Y,Yb,Lu)<sub>2</sub>Si<sub>2</sub>O<sub>7</sub> in the presence of Al(OH)<sub>3</sub> impurities. *J. Eur. Ceram. Soc.* **27**, 2705–2713 (2007).
- Fritsch, M., Klemm, H., Herrmann, M. & Schenk, B. Corrosion of selected ceramic materials in hot gas environment. *J. Eur. Ceram. Soc.* **26**, 3557–3565 (2006).
- Golden, R. A. & Opila, E. J. A method for assessing the volatility of oxides in high-temperature high-velocity water vapor. *J. Eur. Ceram. Soc.* **36**, 1135–1147 (2016).
- Darhout, E. & Gitzhofer, F. Thermal cycling and high-temperature corrosion tests of rare earth silicate environmental barrier coatings. *J. Therm. Spray Technol.* **26**, 1823–1837 (2017).
- Poerschke, D. L., Jackson, R. W. & Levi, C. G. Silicate deposit degradation of engineered coatings in gas turbines: progress toward models and materials solutions. *Ann. Rev. Mater. Sci.* **47**, 16.11–16.34 (2017).
- Levi, C. G., Hutchinson, J. W., Vidal-Setif, M.-H. & Johnson, C. A. Environmental degradation of thermal-barrier coatings by molten deposits. *MRS Bull.* **37**, 932–941 (2012).
- Harder, B. J., Ramirez-Rico, J., Almer, J. D., Lee, K. N. & Faber, K. T. Chemical and mechanical consequences of environmental barrier coating exposure to calcium-magnesium-aluminosilicate. *J. Am. Ceram. Soc.* **94**, S178–S185 (2011).

36. Liu, J., Zhang, L., Liu, Q., Cheng, L. & Wang, Y. Calcium-magnesium-aluminosilicate corrosion behaviors of rare-earth disilicates at 1400 °C. *J. Eur. Ceram. Soc.* **33**, 3419–3428 (2013).
37. Ahlborg, N. L. & Zhu, D. Calcium-magnesium aluminosilicate (CMAS) reactions and degradation mechanisms of advanced environmental barrier coatings. *Surf. Coat. Technol.* **237**, 79–87 (2013).
38. Turcer, L. R., Krause, A. R., Garces, H. F., Zhang, L. & Padture, N. P. Environmental-barrier coating ceramics for resistance against attack by molten calcia-magnesia-aluminosilicate (CMAS) glass: part I,  $YAlO_3$  and  $Y_2Si_2O_7$ . *J. Eur. Ceram. Soc.* **38**, 3905–3913 (2018).
39. Summers, W. D. et al. Roles of composition and temperature in silicate deposit-induced recession of yttrium disilicate. *Acta Mater.* **160**, 34–36 (2018).
40. Stolzenburg, F., Johnson, M. T., Lee, K. N., Jacobson, N. S. & Faber, K. T. The interaction of calcium–magnesium–aluminosilicate with ytterbium silicate environmental barrier materials. *Surf. Coat. Technol.* **284**, 44–50 (2015).
41. Stolzenburg, F. et al. The influence of calcium-magnesium-aluminosilicate deposits on internal stresses in  $Yb_2Si_2O_7$  multilayer environmental barrier coatings. *Acta Mater.* **105**, 189–198 (2016).
42. Zhao, H., Richards, B. T., Levi, C. G. & Wadley, H. N. G. Molten silicate reactions with plasma sprayed ytterbium silicate coatings. *Surf. Coat. Technol.* **288**, 151–162 (2016).
43. Turcer, L. R., Krause, A. R., Garces, H. F., Zhang, L. & Padture, N. P. Environmental-barrier coating ceramics for resistance against attack by molten calcia-magnesia-aluminosilicate (CMAS) glass: part II,  $Yb_2Si_2O_7$  and  $Sc_2Si_2O_7$ . *J. Eur. Ceram. Soc.* **38**, 3914–3924 (2018).



**Open Access** This article is licensed under a Creative Commons Attribution 4.0 International License, which permits use, sharing, adaptation, distribution and reproduction in any medium or format, as long as you give appropriate credit to the original author(s) and the source, provide a link to the Creative Commons license, and indicate if changes were made. The images or other third party material in this article are included in the article's Creative Commons license, unless indicated otherwise in a credit line to the material. If material is not included in the article's Creative Commons license and your intended use is not permitted by statutory regulation or exceeds the permitted use, you will need to obtain permission directly from the copyright holder. To view a copy of this license, visit <http://creativecommons.org/licenses/by/4.0/>.

© The Author(s) 2019